THE JOURNAL OF BIOLOGICAL CHEMISTRY
Vol. 277, No. 22, Issue of May 31, pp. 19905–19912, 2002
Printed in U.S.A.

Molecular Determinants of the Sensory and Motor Neuron-derived Factor Insertion into Plasma Membrane*

Received for publication, February 15, 2002
Published, JBC Papers in Press, March 14, 2002, DOI 10.1074/jbc.M201587200

Hugo Cabedo‡, Carolina Luna§, Asia M. Fernández‡, Juana Gallar§, and Antonio Ferrer-Montiel‡¶

From the ‡Centro de Biología Molecular y Celular and §Instituto de Neurociencias-Consejo Superior de Investigaciones Científicas, Universidad Miguel Hernández, Alicante 03202, Spain

The sensory and motor neuron-derived factor (SMDF) is a type III neuregulin that regulates development and proliferation of Schwann cells. Although SMDF has been shown to be a type II protein, the molecular determinants of membrane biogenesis, insertion, and topology remain elusive. Here we used heterologous expression of a yellow fluorescent protein-SMDF fusion protein along with a stepwise deletion strategy to show that the apolar/uncharged segment (Ile^{76}-Val^{100}) acts as an internal, uncleaved membrane insertion signal that defines the topology of the protein. Unexpectedly, removal of the transmembrane segment (TM) did not eliminate completely membrane association of C-terminal fragments. TM-deleted fusion proteins, bearing the amino acid segment (Ser^{283}-Glu^{296}) located downstream to the epidermal growth factor-like motif, strongly interacted with plasma membrane fractions. However, synthetic peptides patterned after this segment did not insert into artificial lipid vesicles, suggesting that membrane interaction of the SMDF C terminus may be the result of a post-translational modification. Subcellular localization studies demonstrated that the 40-kDa form, but not the 83-kDa form, of SMDF was segregated into lipid rafts. Deletion of the N-terminal TM did not affect the interaction of the protein with these lipid microdomains. In contrast, association with membrane rafts was abolished completely by truncation of the protein C terminus. Collectively, these findings are consistent with a topological model for SMDF in which the protein associates with the plasma membrane through both the TM and the C-terminal end domains resembling the topology of other type III neuregulins. The TM defines its characteristic type II membrane topology, whereas the C terminus is a newly recognized anchoring motif that determines its compartmentalization into lipid rafts. The differential localization of the 40- and 83-kDa forms of the neuregulin into rafts and non-raft domains implies a central role in the protein biological activity.

Neuregulin-1 gene (NRG-1)[1] products comprise a group of cell-cell signaling proteins that act as ligands for the same family of ErbB receptor tyrosine kinases (1). Members of the neuregulin family are expressed in several tissues including nervous system and heart, where they are implicated in diverse cellular processes, such as cell proliferation, differentiation, and survival (2).

The NRG-1 family comprises at least 14 different isoforms, each containing an EGF-like motif that is essential for receptor recognition. NGR-1 isoforms have been classified according to the structure of their N-terminal region. Thus, type I and type II isoforms (which include acetylcholine receptor-inducing activity and glial growth factor II) contain an Ig-like domain, whereas type III presents a cysteine-rich domain (2). In addition, most of the family members are membrane proteins that suffer a proteolytic cleavage to relieve a signaling domain essential for their functional activity (6).

Among the NGR-1 family, the type III subfamily plays a role in the signaling that coordinates the interaction of peripheral nervous system with Schwann cells and muscles (3). The first type III NRG reported was SMDF, a neuregulin highly expressed in motor neurons and dorsal root ganglion neurons (4). At variance with other type III NRGs, SMDF has a type β3 EGF-like motif and is characterized by the absence of a second TM segment downstream of the EGF-like domain. Amino acid sequence and hydropathy analysis does not reveal the presence of a true TM segment (4). There is, however, an apolar/uncharged stretch of amino acids at the N-terminal domain that might act as a TM segment (4, 5). Indeed, SMDF has been proposed to be a group II membrane protein with a single TM segment that locates the N terminus to the cytosol, and exposes the EGF-like motif to the extracellular milieu (5). The mitogenic activity of SMDF on neighboring cells may require the proteolytic release of the EGF-like motif, although the intact protein may also serve as a membrane-attached signal (5, 6). In support of this notion, it has been reported that some members of the NRG-1 family are segregated into lipid rafts, membrane microdomains considered platforms for the selective delivery of proteins to specialized locations in neurons and epithelial cells (7).

In this paper, we study the molecular determinants of SMDF topology. In addition, we investigate whether SMDF biogenesis involves compartmentalization in lipid rafts. The experimental approach uses an YFP-SMDF fusion protein that had the fluorescent protein fused to the N terminus of the NRG. We show that the apolar/uncharged region located at the N-terminal domain of the protein acts as an uncleaved, internal membrane insertion signal sequence, and report that the protein is addi-

* This work was supported by grants from Fundación Navarro Tripodi (to H. C.), La Fundación La Caixa Grant 98/027-00 (to A. F.-M.), Spanish Interministerial Commission of Science and Technology (CICYT) and European Commission Grants SAF-2000-0142 and 1FD97-0662-C02 01 (to A. F.-M.), and CICYT Grant SAF 99-0066-C02-02 (to A. F.-M., and J. G.). The costs of publication of this article were defrayed in part by the payment of page charges. This article must therefore be hereby marked "*advertisement*" in accordance with 18 U.S.C. Section 1734 solely to indicate this fact.

¶ To whom correspondence should be addressed: Centro de Biología Molecular y Celular, Edificio Torregaitán, Universidad Miguel Hernández, Avenida Ferrocarril s/n, 03202 Elche (Alicante), Spain. Tel.: 349-6665-8727; Fax: 349-6665-8758; E-mail: aferrer@umh.es.

[1] The abbreviations used are: NRG-1, neuregulin 1 gene family; DMPC, dimyristoylphosphatidylcholine; EGF, epidermal growth factor; FBS, fetal bovine serum; GFP, green fluorescent protein; GST, glutathione *S*-transferase; PBS, phosphate-buffered saline; SMDF, sensory and motor neuron-derived factor; TM, transmembrane segment; YFP, yellow variant of green fluorescent protein.

tionally anchored to the plasma membrane through its C terminus, probably by an acylation-like post-translational modification. We also report that SMDF partitions into lipid rafts. Interestingly, only the 40 kDa form of SMDF was detected in rafts domains. Removal of the TM did not alter partitioning of the protein into membrane rafts. In contrast, segregation into these lipid microdomains was prevented by deletion of the C-terminal anchoring site. Taken together, our findings are consistent with a membrane topology model for this protein which resembles that proposed for other members of the type III NRG-1 gene subfamily, namely the protein is anchored to the cell membrane through two sites.

EXPERIMENTAL PROCEDURES

Materials—Human dorsal root ganglion (Normal-NCI CGAP PNS1) cDNA library, primers, Dulbecco's modified Eagle's medium, fetal bovine serum, antibiotics, Optiprep, and pcDNA3.1 were obtained from Invitrogen. *Pfu* turbo DNA polymerase and BL21 codon plus *Escherichia coli* strain were from Stratagene. Horseradish peroxidase-conjugated anti-rabbit IgG and anti-mouse IgG secondary antibodies, monoclonal anti-phosphotyrosine clone PT-66, and phosphatidylinositol-specific phospholipase C were obtained from Sigma. pEYFP-C1 and the anti-GFP antibody (Living Colors Aequorea victoria peptide antibody) were from CLONTECH. Streptavidin Alexa 546 was from Molecular Probes. Anti-HRGβ3 antibody was from Santa Cruz. Biotinylated anti-rabbit IgG was from Vector Laboratories. ECL Plus was from Amersham Biosciences.

Amplification and Cloning of SMDF-encoding cDNA—SMDF-encoding cDNA was amplified from a human DRG library by PCR using *Pfu* turbo DNA polymerase and the *Eco*RI restriction site containing primers 5SMDF: CCT TGG AAT TCG ACG ATT TAT and 3SMDF: GTT AAT GTT CGA ATT CGA CAG GC. The amplified fragment was gel purified, *Eco*RI digested, and cloned into the pcDNA 3.1(+) plasmid. Direct and inverse oriented sequences were selected by restriction analysis and verified by automatic sequencing. To clone SMDF into the pEYFP-C1 plasmid, PCR amplification was performed using as template pcDNA-SMDF with the 5′-*Eco*RI restriction site containing primer 5.4SMDF: CAG GCC GAA TTC TGG AGG TGA GCC G and the 3′-*Sal*I restriction site containing primer 3.1SMDF: GAT GCA GCA AGT CGA CAG CAG CAC C. The amplified product was digested with *Eco*RI and *Sal*I and cloned directionally into the pEYFP-C1 plasmid. For the cloning in pGEX-4T1 a similar procedure was used, except the 5′-*Eco*RI restriction site containing primer 5.2SMDF: GCC TTC TTC TGA ATT CGA GCC GAT G was used.

Production of Deletions—To obtain the pEYFP-SMDFΔ108–296 construct, pEYFP-SMDF was truncated at the *Bgl*II site. A similar strategy, but using the *Esp*I site, was used to produce pEYFP-SMDFΔ1–64 and pEYFP-SMDFΔ65–296. All other deletions were obtained by one-step inverse PCR with the proofreading *Pfu* turbo DNA polymerase and two restriction digestions. Briefly, externally oriented primers with PAC1 unique restriction sites were used to amplify the whole construct except the region to be deleted. PCR products were digested (in the amplification buffer) with 20 units of *Dpn*I for 2 h at 37 °C to remove the methylated plasmid templates, subsequently purified, and digested with PAC1. Purified digestions were re-ligated, transformed in DH5α, and selected for kanamycin resistance. More than 95% of the colonies contained the designed deletions as verified by restriction digestion and automatic sequencing.

Cell Lines, Culture, and Transfections—COS-7 cells were cultured in Dulbecco's modified Eagle's medium containing 10% fetal bovine serum. Cells were plated on 2-cm^2 wells at 250,000 cells/well. 20 h later, cells were transfected with 1 μg of plasmid DNA using LipofectAMINE 2000, following the manufacturer's recommendations. To prepare conditioned mediums, cells were serum starved 24 h post-transfection, and the medium was collected 48–72 later. MCF-7 cells were cultured in Dulbecco's modified Eagle's medium containing 10% fetal bovine serum.

Isolation of Plasma Membrane Fractions from Transfected Cells and Immunoblotting—Crude plasma membranes were essentially prepared as described by Schroering and Carey (5) with minor modifications. Briefly, transfected cells were washed with phosphate-buffered saline (PBS) and lysed with buffer A (2 mM $MgCl_2$, 1 mM EDTA, 1 mM phenylmethylsulfonyl fluoride, 20 mM Hepes pH 7.4). Cell lysates were centrifuged at 6,000 × *g*, 4 °C for 10 min to prepare low speed pellet (Pi, containing the plasma membranes) and supernatants (S), which contain the soluble proteins and the remaining membranes. Low speed pellets (Pi) were washed in buffer B (buffer A + 1 M NaCl), incubated for 15 min at 4 °C, centrifuged, and washed with buffer A for desalting. In some experiments, pellets were washed with 50 mM Na_2CO_3, pH 12. Final pellets (P) and supernatants (S), prepared from equivalent amounts of cells, were mixed with β-mercaptoethanol containing SDS sample buffer, heated, and separated by SDS-PAGE. Proteins were electrotransferred onto nitrocellulose membranes, blocked with 10% fat-free skim milk in TBS and incubated with the anti-GFP antibody or the anti-HRGβ3 polyclonal antibody in blocking buffer (1:2,000) for 1 h. Membranes were washed with TBS-Tween (0.3%), incubated with the horseradish peroxidase-conjugated anti-rabbit IgG, and developed with the ECL Plus system.

Tyrosine Phosphorylation Assay—SMDF-induced tyrosine phosphorylation of ErbB receptors was carried out as described by Ho *et al.* (4). Briefly, MCF-7 cells were grown until ≥80% confluence in 24-well plates. Thereafter, cells were serum starved for 2 h and incubated with serum-free, conditioned medium or recombinant SMDF for 15 min at room temperature as indicated. The medium was removed, and cells were harvested with 100 μl of β-mercaptoethanol containing SDS sample buffer. Whole cell extracts were heat denatured, separated by SDS-PAGE, and analyzed by immunoblotting with the monoclonal anti-phosphotyrosine antibody (1:1,000).

In Vivo Immunocytochemistry and Confocal Microscopy—Cells were seeded on poly-L-lysine-coated coverslips at 50–200 × 10^3 cells/well and transfected as indicated previously. The medium was removed, and cells were washed three times for 5 min using PBS with 10% fetal bovine serum (PBS/FBS) at room temperature. Thereafter, cells were incubated with anti-HRGβ3 (1:200) in PBS/FBS at room temperature for 20 min, washed with PBS/FBS three times for 8 min, and incubated with biotinylated anti-rabbit IgG (1:200) in PBS/FBS at room temperature for 20 min. Washes were repeated, and cells were incubated with streptavidin Alexa 546 (1:200) in PBS/FBS, washed in the same conditions, and prepared for *in vivo* fluorescence microscopy in a Zeiss Axiophot microscope using a 20× objective. For confocal microscopy studies, cells were transfected, washed with PBS, and observed *in vivo* with a confocal microscope Olympus Fluoview 300 using a 478 nm argon laser.

Purification of the Recombinant Neuregulin SMDF from E. coli—SMDF-encoding cDNA was cloned in pGEX-4T-1 and transformed in the BL21 codon plus strain. Bacterial cells were grown at 28 °C until reaching 0.6–0.8 *A* (600 nm). Thereafter, cells were induced with isopropyl-1-thio-β-D-galactopyranoside at 0.3 mM for 4 h and pelleted. The pellet was resuspended in PBS and 5 mM dithiothreitol and sonicated. Triton-X100 was added to reach 1% and centrifuged at 10.000 × *g* for 10 min. GST-SMDF was purified from the supernatant with GSH-agarose beads. After extensive washing, GST-SMDF was eluted from the beads with 10 mM GSH in 5 mM dithiothreitol, 150 mM NaCl, 20 mM Tris-HCl, pH 8.8. Protein concentration was calculated with the method of Bradford (8).

Triton X-100 Flotation Experiments—Analysis of detergent-insoluble complexes in flotation gradients was performed following standard protocols (7, 12, 13). Briefly, about 2.5 × 10^6 transiently transfected cells were cooled on ice, washed with PBS, and scraped off in buffer C (150 mM NaCl, 5 mM EDTA, 1 mM phenylmethylsulfonyl fluoride, 0.5% Triton X-100, 20 mM Hepes pH 7.4), passed 10 times through a 29-gauge needle, extracted at 4 °C for 30 min, and brought to 35% Optiprep. One ml of the extract was sequentially overlaid with 8 ml of 30% Optiprep in 0.5× buffer C and 400 μl of buffer C in an SW41 tube. After centrifugation (178,000 × *g* at 4 °C for 4 h), 10 1-ml fractions were collected from the top to the bottom of the gradient; 200 μl of each fraction was precipitated with trichloroacetic acid, pH-neutralized, and analyzed by immunoblotting using the anti-HRGβ3 and anti-GFP antibodies.

Differential Scanning Calorimetry—For differential scanning calorimetry large multilamellar vesicles made from synthetic dimyristoylphosphatidylcholine (DMPC) or DMPC plus cholesterol at 10% molar percentage were used. Dried lipids films obtained from chloroform solutions were suspended in 100 mM NaCl, 10 mM Hepes pH 7.4 to give a final concentration of 1 mM in terms of lipid phosphorus. The resuspended lipids were kept for 90 min above their phase transition temperatures and vortexed. The resulting liposomes were stored overnight at 4 °C to assure a complete hydration of the sample prior to the differential scanning calorimetry measurements. Thermograms were recorded on a high resolution Microcal MC-2 differential scanning microcalorimeter, equipped with a DA-2 digital interface and data collection, as described (14). Lipid dispersions containing the peptides at different molar ratios, and the corresponding buffer in the reference cell were thermally equilibrated in the microcalorimeter, at ≈10 °C for 45 min, before heat was applied. Differences in the heat capacity between the sample and the reference cell were obtained by raising the temperature at a constant rate of 45 °C/h. Transition temperatures and en-

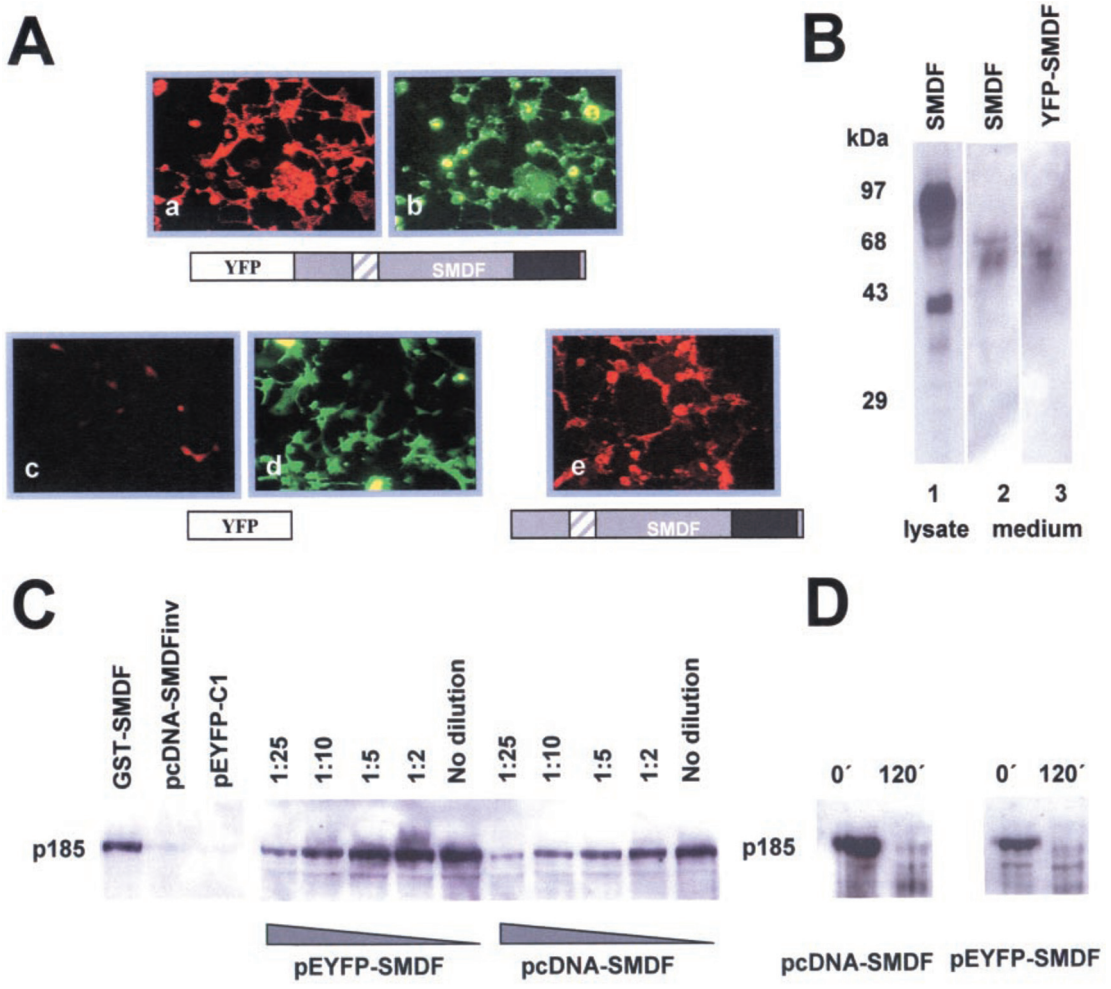

FIG. 1. **Biogenesis and functional activity of SMDF are not altered by the attachment of YFP its N terminus.** *A*, YFP-SMDF (*a* and *b*), YFP (*c* and *d*), and SMDF (*e*) were expressed in COS-7 cells. SMDF and YFP-SMDF produce cell surface immunoreactivity (*a* and *e*), whereas YFP does not (*c*) despite its high level of expression (*d*). Anti-HRGβ3 cell surface immunoreactivity was checked using biotinylated anti-rabbit secondary antibody developed with streptavidin-Alexa 546. A *red* filter (*a*, *c*, and *e*) was used to detect Alexa 546 fluorescence, whereas a *green* filter (*b* and *d*) shows YFP fluorescence. *B*, YFP-SMDF- and SMDF-conditioned culture medium were collected and anti-HRGβ3 immunoreactivity checked by Western blot (*lanes 2* and *3*). Both media produce similar immunoreactivity profiles (a smear $\approx$50 kDa) with faster mobility than the main 83 kDa detected in the cell lysate (*lane 1*). *C*, the MCF-7 p185 phosphorylation-inducing activity of SMDF and YFP-SMDF conditioned media was compared at several dilutions. As shown, no significant differences could be detected. 200 nM recombinant GST-SMDF purified from *E. coli* was used as positive control. *D*, YFP-SMDF and SMDF produce short term effects on the phosphorylation of ErbB receptors. MCF-7 cells were stimulated with SMDF- or YFP-SMDF-conditioned medium, washed, and checked for anti-phosphotyrosine immunoreactivity at 0 and 120 min.

thalpies were calculated by fitting the observed transitions to a single van't Hoff component.

RESULTS

YFP-SMDF Fusion Protein Mimics the Biological Properties of SMDF—To gain insights into SMDF membrane insertion, topology, and localization, we designed a YFP-SMDF fusion protein by cloning the YFP at the N terminus of the neuregulin. For this purpose, the SMDF cDNA was amplified from a human DRG cDNA library and cloned into the pEYFP-C1 vector. The subcelullar location and functional activity of both SMDF and YFP-SMDF were compared upon their transient heterologous expression in COS-7 cells. Immunocytochemical studies using the antibody anti-HGRβ3, raised against the C terminus of the neuregulin, show that both SMDF and YFP-SMDF were highly expressed in the cell surface, as depicted by the labeling of nonpermeabilized COS-7 cells (Fig. 1*A*, *a* and *e*). A pattern of green fluorescence was present in YFP-SMDF- and YFP-transfected cells (Fig. 1*A*, *b* and *d*). As expected, anti-HGR-β3 immunoreactivity was absent in YFP-expressing cells (Fig. 1*Ac*). These results suggest that YFP-SMDF is highly expressed in COS-7 cells and that a fraction of this protein is located in the plasma membrane, with the ectodomain exposed on the cell surface.

SMDF is released into the extracellular medium, presumably by proteolytic processing (4, 5). Membrane release of neuregulins is an important step for their functional activity because it may be required for the efficient interaction with their receptors in target cells (1, 2). Hence, we investigated whether the YFP-SMDF fusion protein was properly processed and released to the extracellular milieu. Immunoblot analysis of culture media from SMDF- and YFP-SMDF-transfected cells disclosed a diffuse, faint band of $\approx$50 KDa which was recognized by the anti-HRGβ3 antibody (Fig. 1*B*, *lanes 2* and *3*). Notice that the molecular mass of this band is smaller than the major, 83-kDa SMDF immunoreactive form observed in cellular lysates (Fig. 1*B*, *lane 1*). Because the antibody recognized the C terminus, these observations indicate that the 50 kDa band corresponds to the C-terminal ectodomain of the neuregulin which contains the EGF-like motif. Thus, the presence of the YFP protein at the N terminus did not affect the proteolytic processing of the neuregulin.

We next evaluated the functional activity of both SMDF and

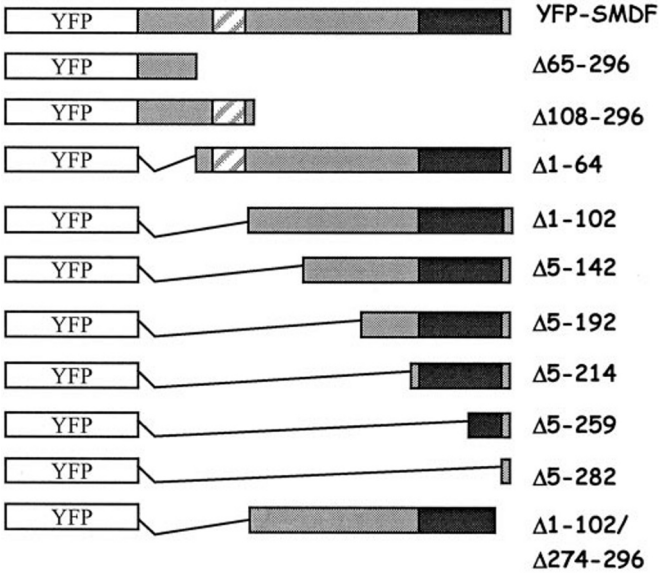

FIG. 2. **Stepwise deletion strategy.** SMDF was cloned in-frame to the C terminus of YFP. *Black boxes* represent the EGF-like domain. The internal hydrophobic sequences are shown as *striped boxes*. Amino acids deleted are indicated for each construct. *Solid lines* denote internal deletion fragments.

YFP-SMDF. For this purpose, we used the epithelial cell line MCF-7, which expresses ErbB receptors (4, 15). Functional activity of the neuregulin was determined as the extent of ErbB tyrosine autophosphorylation induced by conditioned media obtained from COS-7 cells cultures expressing either SMDF or YFP-SMDF. As illustrated in Fig. 1*C*, both types of conditioned medium stimulated the tyrosine phosphorylation of a 185-kDa protein in MCF-7 cells. This band corresponds to the ErbB receptors (4). The extent of receptor phosphorylation decreased as a function of the dilution factor of the conditioned media from both SMDF- and YFP-SMDF-transfected cells (Fig. 1*C*). This functional activity was specific because it was not detected in conditioned media from cells transfected with pEYFP-C1 or an inverted SMDF construct, but it was observed when purified recombinant GST-SMDF was used (Fig. 1*C*). At variance with other neuregulins (16), receptor-induced phosphorylation by both SMDF and YFP-SMDF ectodomains was reversible, as evidenced by the decline of ErbB phosphorylation 2 h after removal of conditioned media (Fig. 1*D*). Taken together, these observations demonstrate that the YFP-SMDF fusion protein reproduces all properties of the wild type III β3 neuregulin.

The Internal Apolar/Uncharged Sequence of SMDF Inserts the Protein into Cell Membranes—SMDF has been proposed to belong to the group II of membrane proteins, having the N terminus facing the cytosol and the C terminus extracellularly exposed (5). The molecular determinants of this topology are still elusive. We addressed this question by evaluating the subcellular location of stepwise deletion mutants carried out on the YFP-SMDF fusion protein (Fig. 2). Because all truncations were carried out on the YFP-SMDF, we will refer to the truncated proteins as the segment deleted, indicating the first and last amino acids removed.

First, we questioned the role of the potential TM domain located in the N terminus segment Ile^{76}-Val^{100}. For this task, we designed two truncated proteins, namely Δ65–296 and Δ108–296, which lack all of the C-terminal ectodomain from residue Glu^{65} and Ser^{108}, respectively. As illustrated in Fig. 3, confocal microscopy images show that deletion mutant Δ108–296 (Fig. 3*b*) exhibited a cell surface labeling pattern identical to that of YFP-SMDF (Fig. 3*a*). Similar results were obtained with the deletion mutant Δ1–64, where the N-terminal domain was deleted up to residue Ala^{64}. In contrast, the N-terminal Δ65–296 and the C-terminal Δ1–101 fragments displayed a distribution of fluorescence similar to that of YFP protein. Thus, removal of the amino acid stretch Ile^{76}-Val^{100} disrupts the insertion of the protein in the plasma membrane.

This finding was substantiated further by biochemical and immunological analysis of subcellular fractions derived from YFP-SMDF full-length and deletion mutants transfected in COS-7 cells. Cell cultures were harvested, lysed, and enriched plasma membrane fractions were pelleted by centrifugation. To prevent contamination with peripheral proteins, plasma membrane fractions were washed with 1.0 M NaCl and/or with pH 12. Under these conditions, YFP was found in the supernatant fraction (Fig 4, P1 and S1), whereas YPF-SMDF was encountered mainly in the pelleted membrane fraction (Fig. 4, P2 and S2), consistent with its location in the cell surface. The Δ108–296 truncated protein was also largely associated with low speed pellet fractions (Fig. 4, P3 and S3). In contrast, deletion mutant Δ65–296 was only detected in the supernatant fraction (Fig. 4, P4 and S4), similar to free YFP. Unexpectedly, Δ101–296, which lacks the TM segment, was found primarily in the plasma membrane-enriched fractions (Fig. 4, P5 and S5), suggesting the presence in this protein of a plasma membrane anchoring domain. Taken together, these findings demonstrate that the internal hydrophobic sequence is an uncleaved, membrane insertion signal sequence and suggest the existence of an additional, previously unrecognized membrane anchoring site in the ectodomain of SMDF.

The C-terminal Sequence of SMDF Behaves as a Membrane-anchoring Domain—Amino acid sequence and hydropathy analysis of the protein domain downstream of the TM segment did not reveal the presence of additional hydrophobic stretches that may explain the ability of C-terminal fragments to associate with membrane fractions. Accordingly, to identify this protein domain we designed additional YFP-SMDF truncated proteins that explore the role of the C-terminal domain (Fig. 2). Deletion mutants were expressed in COS-7 cells, and their subcellular location was investigated with biochemical and immunological methods. As illustrated in Fig. 5, deletion up to Ala^{282} at the end of the EGF-like motif did not eliminate completely membrane interaction of the truncated proteins, as evidenced by the significant presence of the C-terminal fragments Δ5–142, Δ5–214, and Δ5–282 in the plasma membrane-enriched fractions (P1, S1, P2, S2, P3, and S3). This observation suggests that the C-terminal stretch (Ser^{283}-Glu^{296}) is able to anchor a significant portion of the YFP to cellular membranes. In support of this notion, the double truncated fusion protein Δ1–101/Δ274–296, where the TM and the C terminus have been deleted, was not found in the membrane fractions (Fig. 5, P4 and S4). As for Δ5–282, all other truncated proteins containing the segment Ser^{283}-Glu^{296} (Fig. 2) were detected mainly in the pellet fraction. It is interesting to note that immunocytochemical studies on intact cells using the anti-HRGβ3 antibody did not show cell surface expression of the C-terminal fragments (data not shown), indicating an intracellular location of the SMDF ectodomain. This distribution is consistent with confocal fluorescence images, showing a wide cellular distribution pattern (Fig. 3*e*). Collectively, these observations imply that the C terminus of SMDF also functions as a membrane anchoring domain and indicate that the group II topology of the protein is determined by the TM located in the N terminus of the protein.

The C-terminal Segment Does Not Insert into Lipid Bilayers—The amino acid composition and sequence of the segment Ser^{283}-Glu^{296} (SFYSTSTPFLSLPE) is rather polar, containing

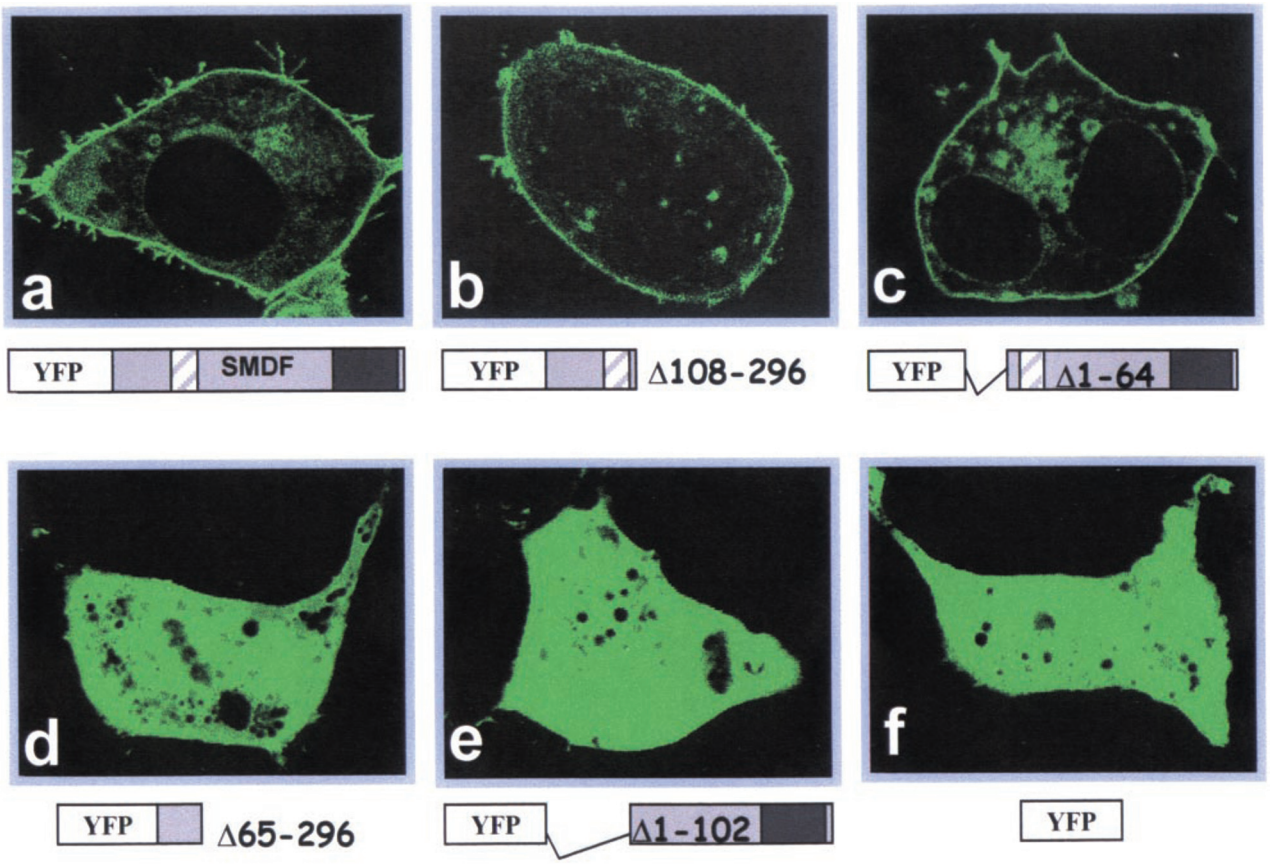

FIG. 3. **Confocal images of YFP-SMDF constructs and stepwise deletions.** Images of COS-7 cells expressing YFP-SMDF show a cortical labeling, indicating plasma membrane localization (*a*). Δ108–296, which lacks the whole extracellular domain but maintains intracellular and internal hydrophobic sequences (*b*), and Δ1–64 (*c*), which lacks the intracellular domain, localize on the plasma membrane. Constructs lacking the internal hydrophobic sequence and or extracellular domain (*d*) or intracellular domain (*e*) show a distribution pattern similar to that of YFP (*f*).

few hydrophobic residues. To evaluate whether this sequence was able to associate with membranes, we studied the interaction of the synthetic peptides WSFYSTSTPFLSLPE and SFYSTSTPWLSLPE with artificial lipid vesicles. Tryptophan residues were included in the sequence to provide intrinsic fluorescence properties to these amino acid sequences. Fluorescence intensity and anisotropy measurements show that both peptides interact marginally with lipid vesicles composed of phosphatidylcholine or phosphatidylcholine/cholesterol (data not shown). Similarly, the thermotropic properties of lipid vesicles made of DMPC and DMPC/cholesterol were not changed significantly by the presence of the synthetic peptides (Fig. 6). Thus, peptides patterned after the SMDF C-terminal domain do not interact with lipid vesicles. This finding suggests that the newly identified membrane anchoring property of this protein domain may be the result of a post-translational modification.

SMDF and YFP-SMDF Are Localized in Lipid Rafts—Members of the neuregulin family have been reported to associate with membrane microdomains rich in cholesterol and sphingomyelin which are insoluble to the detergent Triton X-100, referred to as lipid rafts (7). Association with lipid rafts is an important mechanism of compartmentalization of signaling proteins, especially in neurons (9, 11). Thus, we wondered whether SMDF and YFP-SMDF segregate into these membrane domains. A well known property of proteins inserted in lipid rafts is their insolubility in 1% Triton X-100 at 4 °C and partition in the low density fractions of flotation gradients (10, 18). As depicted in Fig. 7, a significant immunoreactive band of ≈40 kDa was detected with the anti-HGRβ3 antibody in the upper fraction of the Optiprep gradient (Fig. 7*A*). This protein band corresponds to the fast migrating band of SMDF seen in cell lysates (Fig. 1*B*, *lane 1*) (5). SMDF immunoreactivity was not observed in intermediate fractions, but it appeared in the bottom fractions. In these fractions, two distinct bands of ≈40 and ≈83 kDa were detected. Interestingly, the 83-kDa form of the neuregulin was not found in the low density fraction, *i.e.* it was present only in non-rafts domains. Similar results were obtained with YFP-SMDF fusion protein (Fig 7*B*). An anti-HRGβ3 immunoreactive band of ≈70 kDa was detected in the upper gradient fractions. The high density fractions, however, exhibited the presence of two distinct bands of ≈70 and ≈140 kDa, respectively. As for SMDF, the high molecular mass band did not partition into the lipid rafts (Fig 7*B*). Collectively, these findings demonstrate that SMDF is compartmentalized into these membrane domains. It may be possible that two distinct SMDF forms may correspond to monomeric and dimeric species of the protein. However, it was reported that the 83-kDa form was insensitive to chaotropic and reducing agents (5), suggesting a potential post-translational modification of the neuregulin.

YFP Fusion Proteins Containing the C-terminal Sequence of SMDF Are Segregated into Lipid Rafts—To learn which of the SMDF membrane anchoring domains is responsible for the segregation of the protein into lipid rafts, we investigated the interaction of the truncated fusion proteins Δ5–282 containing the C terminus, and the Δ108–296 having the N-terminal TM segment with these membrane microdomains. As depicted in Fig. 7*C*, removal of TM domain did not prevent the association of the truncated fusion protein Δ5–282 with lipid rafts (note that a protein band of ≈32 kDa is present in the low density fraction in *lane 1*). In contrast, we were unable to detect

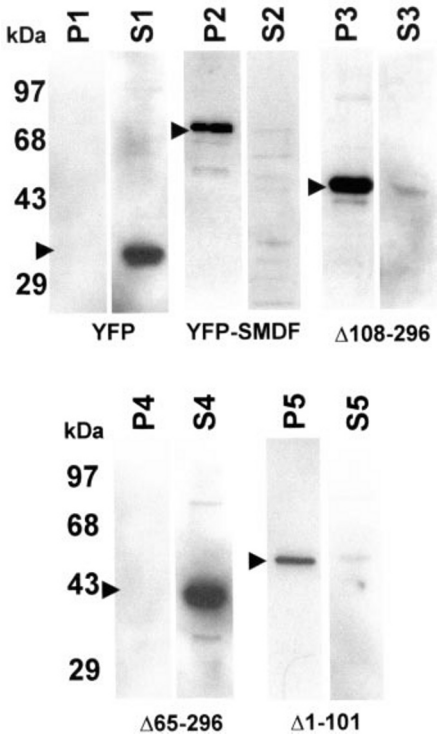

FIG. 4. **Subcellular localization of YFP-SMDF and truncated proteins.** Crude plasma membranes (P) and low speed supernatants (S) were prepared from COS-7 cells expressing YFP, YFP-SMDF, Δ108–296, Δ65–296, and Δ1–101. As expected, YFP is not found on plasma membranes (P1) and is detected on soluble fractions (S1). YFP-SMDF and Δ108–296 are clearly associated with plasma membrane-enriched fractions (P2 and P3) and barely detected in low speed supernatants (S2 and S3). The internal apolar uncharged sequence lacking construct Δ65–296 is not detected on plasma membranes (P4) and is detected in supernatants (S4). Unexpectedly, Δ1–101, which also lacks the internal apolar uncharged sequence but retains the extracellular domain, is attached to membranes.

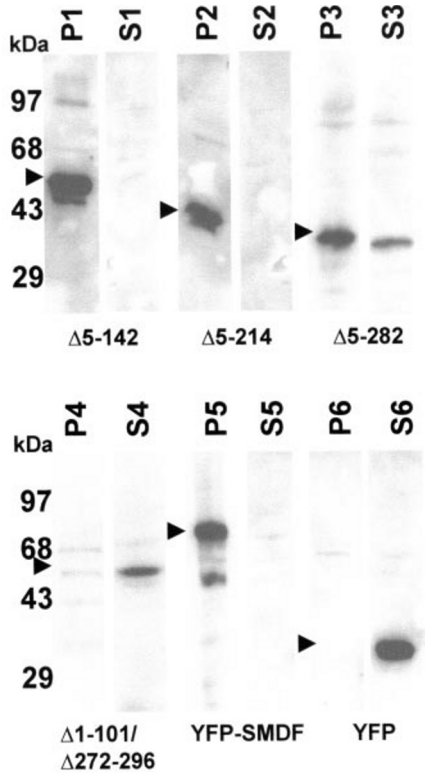

FIG. 5. **C-terminal sequences of SMDF are able to localize YFP in biological membranes.** Portions of the C-terminal domain of SMDF were fused to YFP and expressed in COS-7 cells. Crude membranes (P) and supernatants (S) were prepared and tested for immunoreactivity against YFP. Constructs retaining the 14 C-terminal amino acids of SMDF were able to attach YFP to the membranes (Δ5–142, P1 and S1; Δ5–214, P2 and S2; Δ5–282, P3 and S3). Removing these amino acids localized YFP in the supernatant fraction (P4 and S4). As expected, YFP-SMDF was localized in membranes (P5 and S5) and YFP in the supernatants (P6 and S6).

the C-terminal truncated fusion protein Δ108–296, as well as YFP, in these membrane microdomains (Fig. 7, *D* and *E*). These findings demonstrate that the C-terminal domain is responsible for the segregation of SMDF into membrane rafts.

DISCUSSION

SMDF is a TM neuregulin expressed on the plasma membrane with the active, C-terminal, EGF-like domain oriented to the extracellular space, thus showing a group II membrane protein topology. This membrane arrangement appears to be the result of its unique domain organization among the NRG-1 gene family (5). Instead of a cleavable signal peptide and a clear hydrophobic segment, SMDF contains an uncharged/apolar stretch of amino acids at the N terminus which could serve as an internal, uncleaved signal for membrane association (4). Indeed, our results provide experimental support to this notion, as evidenced by the absence of membrane insertion of truncated SMDF forms that lack this protein segment and the C-terminal domain. Unexpectedly, TM-deleted SMDF species that contain the C terminus of the protein were tightly associated with cellular membranes. These truncated forms were detected in low speed pellets enriched in plasma membrane fractions and were resistant to 1 M NaCl and pH 12 extraction. Furthermore the stepwise deletion analysis identified the C-terminal segment after the EGF-like domain as the anchoring site because removal of this amino acid stretch along with the TM gave rise to non-plasma membrane SMDF species. Thus, our findings are consistent with the existence of two membrane interacting sites on the SMDF neuregulin: a previously proposed N-terminal apolar region comprising Ile^{76}-Val^{100}, and a newly recognized C-terminal site encompassing Ser^{283}-Glu^{296}.

Our observations uncover the molecular determinants of the type II topology characteristic of this protein. Immunocytochemical analysis using the anti-HGRβ3 antibody demonstrates that deletion of the TM resulted in a change in the topology of the protein from N_{int}/C_{out} to N_{int}/C_{int}. In marked contrast, truncation of the newly identified C-terminal region did not alter the topological orientation of the protein. Therefore, the TM domain acts as an internal membrane insertion signal that determines the protein group II membrane topology, whereas the C terminus serves as an additional membrane anchoring domain. These findings call for a revision of the currently accepted topological model of SMDF. The new model substantiates the notion that SMDF has two membrane interacting domains, one defined by the TM in the N terminus and the other determined by the anchor of the C terminus (Fig. 8). This membrane organization is similar to that exhibited by other members of the neuregulin family such as type I β1a and type III β1a (6), thus suggesting a conserved membrane topology. Furthermore, our results imply that the type I neuregulin glial growth factor II, which lacks a TM but displays a C-terminal segment akin to that of SMDF, may also be anchored to cell membranes through its biogenesis.

Because the amino acid sequence of the C terminus of SMDF is highly polar (SFYSTSTPFLSLPE), it is unlikely that this motif integrates into the plasma membrane. Consistent with this notion, synthetic peptides patterned after the C-terminal domain failed to insert into lipid vesicles. Accordingly, a central

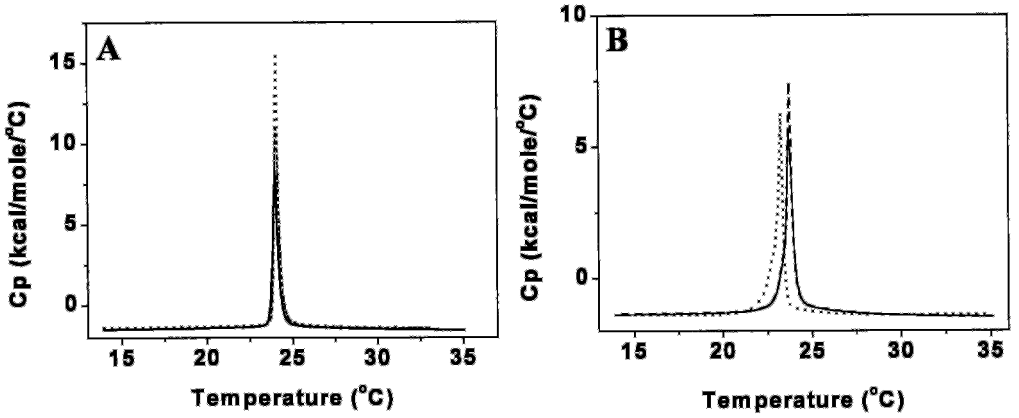

FIG. 6. **The C terminus of SMDF does not insert into lipid bilayers.** Differential scanning calorimetry thermograms of DMPC (*A*) or DMPC/cholesterol (*B*) large multilamellar vesicles alone or in the presence of increasing concentrations of C-terminal peptide of SMDF at lipid:peptide molar ratios of 20:1 and 5:1. The estimated phase transitions enthalpies in vesicles of pure DMPC were 5.4 kcal/mol in the absence of peptide, 5.9 kcal/mol for a 5:1 lipid:peptide ratio, and 5.8 kcal/mol for a 20:1 lipid:peptide ratio. Similarly, for DMPC/cholesterol the values were 4.7 (lipid), 4.8 (5:1 lipid:peptide), and 4.7 kcal/mol (20:1 lipid:peptide).

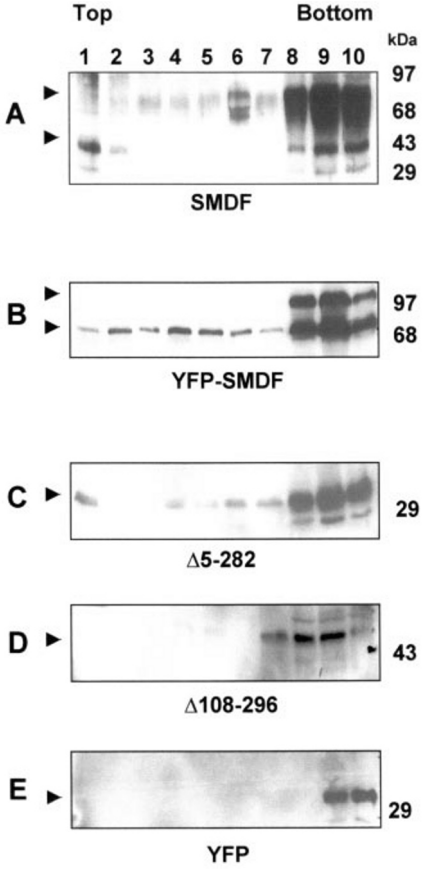

FIG. 7. **SMDF is localized in lipid rafts.** *A*, a band of ≈40 kDa was found in the top fractions of the SMDF wild type-expressing cells, whereas a prominent band of ≈83 kDa joined with a minor band of ≈40 kDa was in the bottom fractions. *B*, in the YFP-SMDF gradients, a band of ≈70 kDa was found in the raft and non-raft fractions, whereas a ≈140 kDa band was detected only in the Triton X-100-soluble fractions. *C*, the 14 C-terminal amino acids of SMDF are able to localize YFP in the lipid rafts. *D*, YFP-SMDFΔ 108–296 was not detected in the top fractions as is the case with YFP (*E*). COS-7 cells were transfected with wild type SMDF (*A*), YFP-SMDF (*B*), Δ5–282 (*C*), Δ108–296 (*D*), or YFP (*E*), extracted with Triton X-100 at 4 °C, and centrifuged in Optiprep density gradients. 10 fractions were collected from the top and analyzed by immunoblotting with anti-HRGβ3 (*A*, *B*, and *C*) or anti-GFP antibodies (*D* and *E*).

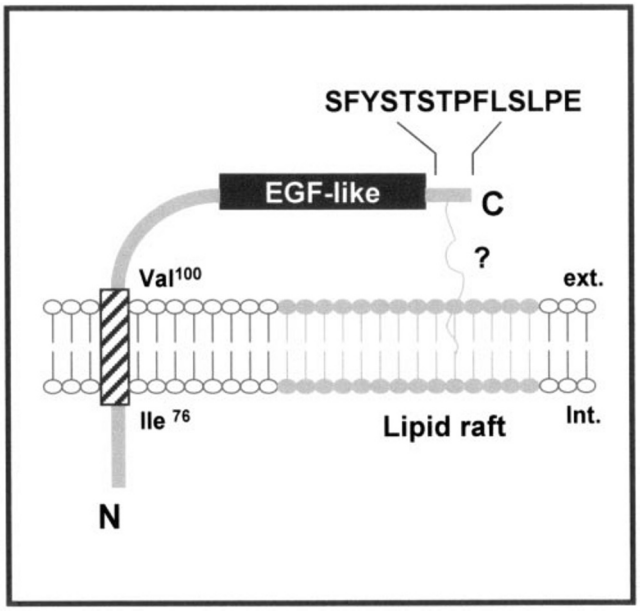

FIG. 8. **Topological model proposed for SMDF.** Internal hydrophobic sequence (*striped box*) determines the membrane insertion of the N-terminal domain of SMDF, whereas an yet unknown post-translational modification anchors the C-terminal end of the protein to the lipid rafts.

question arises: How does the C terminus of the protein associate with membranes? A plausible mechanism is to consider that the protein motif suffers a post-translational modification such as glycosylphosphatidylinositol acylation (22). However, there is no recognizable GPI anchoring motif in the SMDF amino acid sequence. In addition, treatment of membrane fractions containing TM-truncated SMDF proteins with phosphatidylinositol-specific phospholipase C, an enzyme that removes GPI anchors, did not abolish membrane association (data not shown). Thus, alternative post-translational mechanisms should be considered. For example, the C terminus of SMDF might be acylated with cholesterol, an unusual protein modification that plays a key role in hedgehog signaling in *Drosophila* (23, 24). These proteins associate with lipids in part because of a cholesterol modification at their C-terminal ends which occurs during their maturation. This sort of lipid modification has not been described for any other proteins, and therefore consensus sequences have not been established yet (23). The segregation of the SMDF C terminus into lipid microdomains rich in cholesterol is compatible with this hypothesis. Alternatively, SMDF association to lipid rafts may be mediated by *O*-glycosylation of one of the potential *O*-linked sites present in

its C terminus. In support of this notion, it has been described that *O*-glycosylation may play a role in sorting of proteins through association with lipid rafts (17). Clearly, further experimental work is necessary to define the post-translational modification of SMDF C-terminal end that is responsible of membrane insertion.

Recent evidence has shown that type I β1a and type III β1a NRGs are segregated into specialized membrane microdomains rich in sphingomyelin and cholesterol (7). Indeed, lipid rafts play a central role in axonal sorting of membrane proteins in neurons (9). Accordingly, membrane compartmentalization of SMDF may have important functional consequences. For instance, SMDF could be located in the axon where it may have an action on Schwann cell proliferation, as well as in mature neuromuscular junctions where it could promote reinnervation of muscle fibers by motor neurons after nerve damage (4). Thus, we first questioned whether SMDF is also inserted in rafts microdomains and second, what was the role of each membrane interacting site in the protein. SMDF wild type, as well as YFP-SMDF fusion protein were resistant to 1% Triton X-100 extraction, suggesting their interaction with lipid rafts. This tenet was demonstrated unquivocally by Optiprep floating gradients that showed that a significant fraction of SMDF forms in the low density fractions, a hallmark of protein association with membrane rafts and not with cytoskeleton or other subcellular structures (19–21). It is interesting to note that only the 40-kDa form of SMDF wild type was found located in lipid rafts. The higher molecular mass form of the protein, however, was not detected in these lipid microdomains. Similarly, the 70-kDa form of YFP-SMDF, but not the 140-kDa form, was segregated into membrane rafts. Noteworthy, this observation is in agreement with previous reports that found the 83 kDa band in the Triton X-100-soluble fraction (5). The distinct membrane compartmentalization of the two SMDF forms may be a regulatory strategy of protein biogenesis. In support of this notion, the 83-kDa form was found to be accessible to biotin labeling and trypsin proteolysis in nonpermeabilized cells, suggesting that the 83-kDa form is the main cell surface protein, whereas the 40-kDa form would be located primarily in intracellular membranes (5). Hence, segregation into rafts would be necessary for the correct post-translational modification and/or assembly, as well as for sorting and trafficking of SMDF. Alternatively, raft association may play a role in NRG signaling. For example, in neurons it has been found that raft proteins are located primarily in axons, whereas non-raft proteins are targeted to soma and dendrites (9). Interestingly, heterodimer ErbB-2 with ErbB-3 is the active receptor in proliferation of Schwann cells that involve neuronal axons (1). Because the ErbB-2 receptor does not have an EGF binding domain, it is tempting to speculate that the 40-kDa form of SMDF could act as a ligand of the ErB-2/ErB-3 heterodimer. In contrast, the 83-kDa form of SMDF could interact with the two binding sites present in the homodimeric ErbB3/ErbB3 receptors. Hence, membrane compartmentalization between rafts and non-rafts could define distinct biological activities for axonal and somatodendritic SMDF. Future data should decipher the precise biological role of the proposed polarized distribution of SMDF and other neuregulin that also segregate into membrane rafts.

Analysis of the structural requirements that target SMDF to lipid rafts revealed that the C-terminal anchoring domain was a critical determinant for raft association. Indeed, deletion of the N-terminal domain including the TM segment did not alter the partitioning of the neuregulin into lipid raft fractions. In contrast, truncation of the C terminus of the protein completely abolished its segregation into the specialized membrane microdomains. In agreement with these findings, it was reported that although the C-terminal fragment of type III β1a is partially localized in lipid rafts, little of the N-terminal fragment is found in these membrane microdomains (7). Therefore, the membrane-anchoring segment downstream of the EGF-like motif determines the association with lipid rafts.

In summary we have demonstrated that the type III β3 neuregulin is associated with cellular membranes through its N-terminal and C-terminal domains, thus providing a revised membrane model for this protein. The N-terminal TM segment defines the group II membrane topology of the protein, whereas the C terminus determines the segregation of the protein into lipid rafts.

Acknowledgments—We are indebted to Carlos Belmonte (IN-CSIC) for support, Rosa Planells-Cases (University of Hamburg) for insightful comments, and to Consuelo Martínez-Moratalla for technical assistance. Carolina Luna is a predoctoral fellow from UPSA.

REFERENCES

1. Burden, S., and Yarden, Y. (1997) *Neuron* **18,** 847–855
2. Buonano, A., and Fisbach, G. D. (2001) *Curr. Opin. Neurobiol.* **11,** 287–296
3. Wolpowitz, D., Mason, T. B. A., Dietrich, P., Mendelsohn, M., Talmage, D. A., and Role, L. W. (2000) *Neuron* **25,** 79–91
4. Ho, W. H., Armanini, M. P., Nuijens, A., Philips, H. S., and Osheroff, P. L. (1995) *J. Biol. Chem.* **270,** 14523–14532
5. Schroering, A., and Carey, J. (1998) *J. Biol. Chem.* **273,** 30643–30650
6. Wang, J. Y., Miller, S. J., and Falls, D. (2001) *J. Biol. Chem.* **276,** 2841–2851
7. Frenzel, K. E., and Falls, D. L. (2001) *J. Neurochem.* **77,** 1–12
8. Bradford, M. M. (1976) *Anal. Biochem.* **72,** 248–254
9. Ledesma, M. D., Simons, K., and Dotti, C. (1998) *Proc. Natl. Acad. Sci. U. S. A.* **95,** 3966–3971
10. Brown, D. A., and London, E. (2000) *J. Biol. Chem.* **275,** 17221–17224
11. Galbiati, F., Razani, B., and Lisanti, M. P. (2001) *Cell* **106,** 403–411
12. Mañes, S., Mira, E., Gómez-Moutón, C., Lacalle, R. A., Séller, P., Labrador, J. P., and Martínez-A, C. (1999) *EMBO J.* **18**, 6211–6220
13. Lafont, F., Verkade, P., Galli, T., Wimmer, C., Louvard, D., and Simons, K. (1999) *Proc. Natl. Acad. Sci. U. S. A.* **96,** 3734–3738
14. Encinar, J. A., Fernández, A. M., Gavilanes F., Albar, J. P., Ferragut, J. A., and Gonzalez-Ros, J. M. (1996) *Biophys. J.* **71,** 1313–1323
15. Osheroff, P. L., Tsai, S. P., Chiang, N. Y., King, K. L., Li, R., Lewis, G. D., Wong, K., Henzel, W., and Mather, J. (1999) *Growth Factors* **16**, 241–253
16. Li, Q., and Loeb, J. A. (2001) *J. Biol. Chem.* **276,** 38068–38075
17. Alfalah, M., Jacob, R., Preuss, U., Zimmer, K. P., Nain, H., and Naim, H. Y. (1999) *Curr. Biol.* **9,** 593–596
18. Ikonen, E. (2001) *Curr. Opin. Cell Biol.* **13,** 470–477
19. Brown, D. A., and Rose, J. K. (1992) *Cell* ***68,*** 533–544
20. Johnston, J. A., Ward, C. L., and Kopito, R. R. (1998) *J. Cell Biol.* **143,** 1883–1898
21. Kennedy, M. B. (1997) *Trends Neurosci.* **20,** 264–268
22. Muñiz, M., and Riezman, H. (2000) *EMBO J.* **19,** 10–15
23. Ingham, P. W. (2001) *Science* **294,** 1879–1881
24. Rietveld, A., Neutz, S., Simons, K., and Eaton S. (1999) *J. Biol. Chem.* **274,** 12049–12054